



**HAL**  
open science

# Wave turbulence in a two-layer fluid: coupling between free surface and interface waves

Bruno Issenmann, Claude Laroche, Eric Falcon

► **To cite this version:**

Bruno Issenmann, Claude Laroche, Eric Falcon. Wave turbulence in a two-layer fluid: coupling between free surface and interface waves. EPL - Europhysics Letters, 2016. hal-01382922v1

**HAL Id: hal-01382922**

**<https://hal.science/hal-01382922v1>**

Submitted on 18 Oct 2016 (v1), last revised 24 Jan 2017 (v2)

**HAL** is a multi-disciplinary open access archive for the deposit and dissemination of scientific research documents, whether they are published or not. The documents may come from teaching and research institutions in France or abroad, or from public or private research centers.

L'archive ouverte pluridisciplinaire **HAL**, est destinée au dépôt et à la diffusion de documents scientifiques de niveau recherche, publiés ou non, émanant des établissements d'enseignement et de recherche français ou étrangers, des laboratoires publics ou privés.

---

# Wave turbulence in a two-layer fluid: coupling between free surface and interface waves

BRUNO ISSENMANN<sup>1,2</sup>, CLAUDE LAROCHE<sup>1</sup> and ERIC FALCON<sup>1</sup>

<sup>1</sup> *Université Paris Diderot, Sorbonne Paris Cité, MSC, UMR 7057 CNRS - F-75013 Paris, France*

<sup>2</sup> *Univ Lyon, Université Claude Bernard Lyon 1, CNRS, Institut Lumière Matière, F-69622, Villeurbanne, France*

PACS 47.35.i – Hydrodynamic waves  
PACS 05.45.a – Nonlinear dynamics and chaos  
PACS 47.27.-i – Turbulent flows  
PACS 47.55.-t – Multiphase and stratified flows

**Abstract** – We experimentally study gravity-capillary wave turbulence on the interface between two immiscible fluids of close density with free upper surface. We locally measure the wave height at the interface between both fluids by means of a highly sensitive laser Doppler vibrometer. We show that the inertial range of the capillary wave turbulence regime is significantly extended when the upper fluid depth is increased: The crossover frequency between the gravity and capillary wave turbulence regimes is found to decrease whereas the dissipative cut-off frequency of the spectrum is found to increase. We explain most of these observations by the progressive decoupling between waves propagating at the interface and the ones at the free surface, using the full dispersion relation of gravity-capillary waves in a two-layer fluid of finite depths.

---

**Introduction.** – Stratified fluids are ubiquitous in Nature such as in ocean or in atmosphere. The density stratification is usually due to a temperature or salinity gradient with the depth in oceans, or a temperature or humidity gradient with altitude in the atmosphere. The simplest stratified fluid consists in two superimposed homogeneous fluids, the fluid with higher density being below the fluid with lower density. In this situation, waves can propagate at the interface between the two fluid layers but also at the free surface of the top one. Under certain conditions, surface and interface waves interact together [1, 2]. An astonishing manifestation of this phenomenon is the dead-water effect first observed in 1904 on the sea surface [3], and recently reproduced in experiments [4, 5]. Indeed, ships evolving on a calm sea can slow or even stop sailing in a two-layer fluid due to the extra-drag generated by large interface waves. The coupling between the surface and interface waves in a two-layer fluid also generates narrow nested V-shaped wakes observed behind ships [6, 7], as well as the damping of ocean surface waves over a layer of fluid mud [8]. Such a coupling is also involved in Faraday instability of floating droplets on a liquid bath [9, 10], or during the long-wave instabilities in ultra thin two-layer liquid films ( $< 100$  nm) in chemical physics [11]. In industrial applications like metal refining, such inter-

actions can also have an influence on the ripples created during dewetting [12]. At last, the coupling between the surface and interface waves of large amplitudes occur in many physical and biological situations (involving or not elasticity), and lead to numerous challenging studies in applied mathematics such as the predictions of new solitary waves [13, 14].

When a set of stochastic waves, propagating on a free surface, have large enough amplitudes, nonlinear interactions between waves can generate a wave turbulence regime. These nonlinear interactions transfer the wave energy from the large scales, where it is injected, to the small scales where it is dissipated. This generic phenomenon concerns various domains at different scales: Surface and internal waves in oceans, elastic waves on plates, spin waves in solids, magnetohydrodynamic waves in astrophysical plasma (for reviews, see refs. [15–18]). Weak turbulence theory was developed in the 60’s [19–21], and leads to predictions on the wave turbulence regime in almost all domains of physics involving waves [16, 17]. The past decade has seen an important experimental effort to test the validity domain of weak turbulence theory on different wave systems (e.g. hydrodynamics, optics, hydro-elastic or elastic waves) [22].

In this paper, we study gravity-capillary wave turbu-

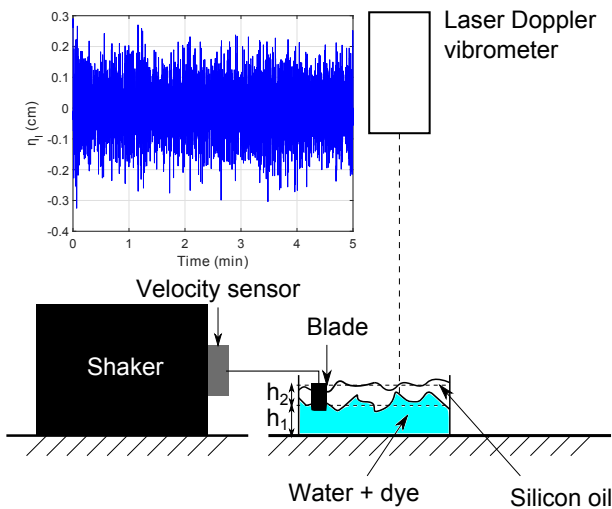


Fig. 1: Experimental setup. Free surface and interfacial waves are generated by a wavemaker. Lower fluid: water (depth at rest  $h_1$ ). Upper fluid: silicon oil (depth at rest  $h_2$ ). Dashed lines: interface and free surface at rest. A laser vibrometer locally measures the height of the interface, the water being dyed with white paint. Inset: Typical evolution of the interfacial wave height  $\eta_I(t)$  as a function of time.  $h_2 = 0.9$  cm.

lence on the interface of a two-layer fluid with free upper surface. Waves propagate both at the interface and at the free surface (either in phase or in antiphase), and this coupling depends strongly on the upper fluid depth. When this depth increases, we show that these two modes become progressively uncoupled explaining thus most of the observations on the wave turbulence spectra. When the upper fluid is deep enough, the two modes are then fully uncoupled, leading to the observation of a spectrum of purely capillary interfacial wave turbulence on two decades in frequency, fluids being of almost same density. The article is organized as follows. We will first describe the experimental setup, then the experimental results and the model, before comparing them to each other.

**Experimental setup.** – The experimental setup is sketched in fig. 1. Two fluids are placed in a circular 22 cm diameter plastic vessel. The lower fluid is water, and the upper fluid is a silicon oil (10 cSt PDMS DC200). Their depths at rest are respectively  $h_1$  and  $h_2$ .  $h_1 = 4.3$  cm is fixed whereas  $h_2$  is varied between 0 and 0.9 cm, thus  $0 \leq h_2/h_1 < 21\%$ . Their kinematic viscosities are respectively  $\nu_1 = 10^{-6}$  m<sup>2</sup>/s and  $\nu_2 = 10^{-5}$  m<sup>2</sup>/s. Their densities are respectively  $\rho_1 = 1000$  kg/m<sup>3</sup> and  $\rho_2 = 935$  kg/m<sup>3</sup> leading to a small Atwood number  $A = (\rho_1 - \rho_2)/(\rho_1 + \rho_2) = 0.033$ . The surface tension values are respectively  $\gamma_w = 72$  mN/m for water/air,  $\gamma_S = 20$  mN/m for silicon oil/air [23]. The interfacial tension between water and silicon oil is  $\gamma_I = 25$  mN/m [24].

An electromagnetic shaker (LDS V406/PA 100E) horizontally vibrates a plexiglas blade that generates gravity-capillary waves at the interface between both fluids and at

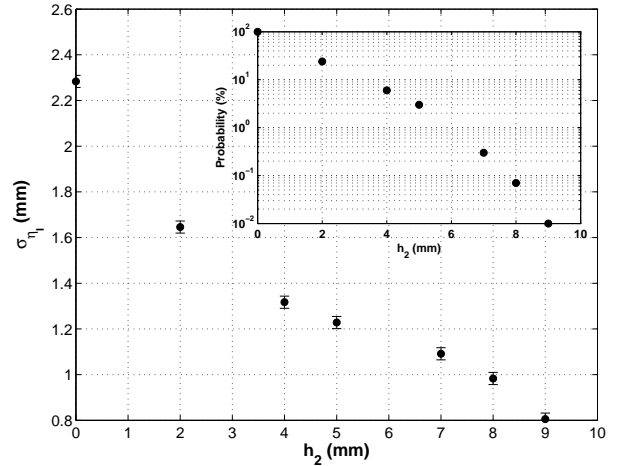


Fig. 2: rms height of the interfacial waves as a function of the upper fluid depth at rest,  $h_2$ . Inset: Probability for the interfacial waves to emerge from the free surface of the upper fluid as a function of its depth,  $h_2$ .  $\sigma_{\eta_s}(h_2 = 0) = 2.3$  mm

the free surface. The immersed part of the blade is fixed to 2 cm regardless of  $h_2$ . The shaker is driven with a random forcing in amplitude and frequency between 0.1 Hz and 6 Hz. The rms amplitude and velocity of the blade is fixed to respectively 5 mm and 5 cm/s, regardless of the experiment presented here. A home made velocity sensor [25] is fixed to the shaker axis to measure the instantaneous blade velocity  $V(t)$ .

A laser Doppler vibrometer (Polytec OFV506) placed above the setup measures the vertical velocity of the interface deformation at one point given by the position of the vertical laser beam (see fig. 1). To wit, white dye is added to the water bulk to make it slightly diffusing (concentration around 1% in volume). The velocity is extracted from the interference between the incident beam and the light back scattered by the diffusing fluid. After temporal integration, one thus obtains the interface height  $\eta_I(t)$ . The laser Doppler vibrometer has an accuracy of order of 10  $\mu$ m. To avoid direct transmitted vibration from the shaker to the vibrometer, the latter is mechanically uncoupled from the shaker. Signals are then high-pass filtered ( $> 0.5$  Hz) to avoid possible residual low-frequency vibrations. They are acquired for  $T = 5$  minutes (or 30 minutes to converge statistics to compute the probability density function (PDF) of the wave height). Note that the white dye added to water certainly modifies its surface tension  $\gamma_w$  and its viscosity but their orders of magnitudes remain valid. We will thus use their above values in the model below.

**Experimental results.** – A temporal recording of the interfacial wave height  $\eta_I(t)$  is shown in the inset of fig. 1. It displays an erratic behavior in response to the stochastic forcing. As shown in fig. 2, the root-mean-square (rms) value of the interface wave height  $\sigma_{\eta_I} \equiv \sqrt{\langle \eta_I^2(t) \rangle}$  is found to decrease strongly when the depth

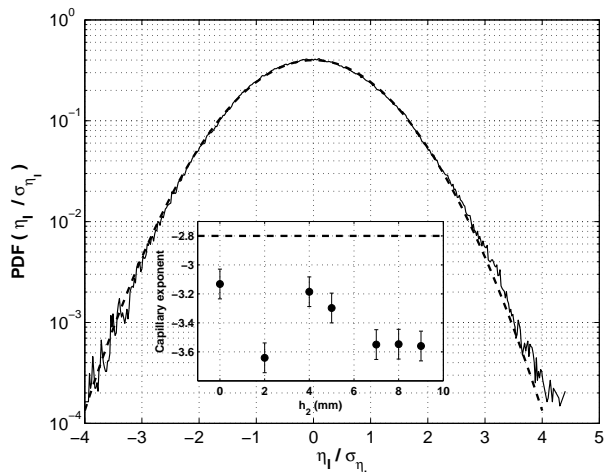


Fig. 3: Solid line: Probability density function of the rescaled interfacial wave height,  $\eta_I/\sigma_{\eta_I}$ . Dashed line: Gaussian with zero mean and unit standard deviation.  $h_2 = 4$  mm.  $\sigma_{\eta_I} = 1.32$  mm. Inset: Frequency-power law exponents of the capillary spectrum as a function of  $h_2$ . Dashed line: Theoretical value ( $-17/6$ ) of the frequency-power law exponent of capillary wave turbulence.

of the upper fluid,  $h_2$ , is increased. Temporal average is denoted by  $\langle \cdot \rangle$ . The probability density function (PDF) of the rescaled interface wave height,  $\eta_I/\sigma_{\eta_I}$ , is closed to a Gaussian (see fig. 3), and is found independent of  $h_2$  (not shown).

Assuming that the distribution of free surface wave height,  $\eta_S$ , is also Gaussian, we infer that the PDF of their height difference,  $\eta_I - \eta_S$ , is also close to a Gaussian of standard deviation  $\sigma_{diff} = \sqrt{\sigma_{\eta_I}^2 + \sigma_{\eta_S}^2}$ . We can then easily compute the probability to have  $\eta_I - \eta_S$  larger than  $h_2$ , that quantifies the probability for the lower fluid to emerge from the upper fluid layer. Since the prescribed rms velocity of the blade is kept constant for all the experiments, we assume  $\sigma_{\eta_S}(h_2)$  to be constant regardless of  $h_2$ , and equal to its value measured for  $h_2 = 0$ , i.e.  $\sigma_{\eta_S}(h_2) = 2.3$  mm, both fluids being incompressible and viscous effects negligible at large scales (see below). Those probabilities are displayed in the inset of fig. 2, and show that lower fluid rarely emerges from the upper fluid layer, for most of our experiments. It is thus relevant to consider a continuous upper fluid layer with no interfacial crest emerging from the upper layer. Note that this is not true for the smallest depth used,  $h_2 = 2$  mm since this probability reaches 24%.

From the temporal recording of the interface wave height,  $\eta_I(t)$  (see inset of fig. 1), one computes its power spectrum density as the square modulus of the Fourier transform of  $\eta_I(t)$  over a duration  $T$ :  $S_{\eta_I}(f) \equiv |\int_0^T \eta_I(t) e^{i\omega t} dt|^2 / (2\pi T)$ , where  $\omega = 2\pi f$ . Figure 4 shows the power spectra of the interface wave height when the upper fluid depth increases. For  $h_2 = 0$  mm (bottom curve), the usual gravity-capillary wave turbulence spec-

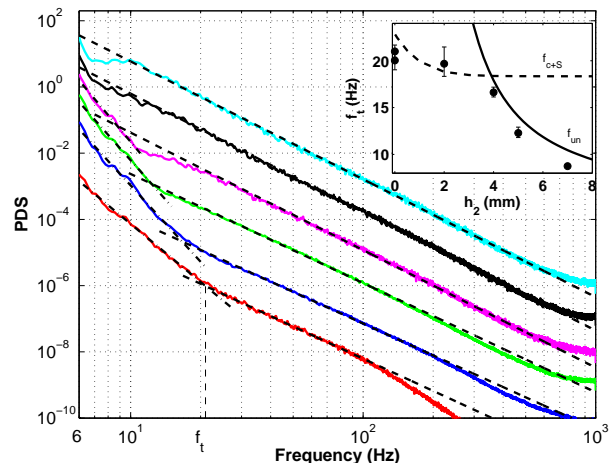


Fig. 4: (color online) Power spectrum density of the interface wave height,  $S_{\eta_I}(f)$ , for increasing upper fluid depths  $h_2 = 0$  (red), 4 (blue), 5 (green), 7 (magenta), 8 (black) and 9 mm (cyan) (from bottom to top, shifted vertically for clarity). The dashed (resp. dash-dotted) lines are the best power-law fits of the capillary (resp. gravity) wave turbulence regimes. Forcing frequencies  $\leq 6$  Hz. Inset: Experimental crossover frequency  $f_t$  between gravity and capillary regimes as a function of  $h_2$  (symbols). Dashed line: theoretical crossover frequency  $f_{c+S}$  (see text). Solid line: frequency  $f_{un}$  for which the interface and free surface waves of the mode + become uncoupled (i.e.  $\eta_I/\eta_S = 1/10$  - see fig. 7).

trum is observed as previously found in several recent studies [26–30]. Up to a cutoff frequency at  $\approx 100$  Hz, related to dissipation, this spectrum is consistent with two different power-law regimes for frequencies above  $f_t \approx 20$  Hz (capillary regime) and below  $f_t$  (gravity regime) as expected by the weak turbulence theory [16, 17] and already observed experimentally [26–30]. Note that the exponent of the capillary regime is slightly lower than its predicted value  $-17/6$  (inset of fig. 3). The crossover frequency  $f_t$  between gravity and capillary wave turbulent regimes is linked to the capillary length  $l_{cw} = \sqrt{\gamma_w/\rho_1 g}$  [26]. When  $h_2$  is increased, the capillary regime is found to hold down to lower and lower frequencies (see curves from  $h_2 = 4$  to 7 mm in fig. 4), until no transition is clearly visible before reaching the forcing frequencies (see curves for  $h_2 \geq 8$  mm). This crossover frequency  $f_t$  is found to decrease up to a factor 2.5 (from 20 to 8 Hz, see inset of fig. 4) when  $h_2$  is increased. Moreover, the cut-off frequency increases of a factor 7 (roughly from 100 to 700 Hz) when  $h_2$  is increased. This leads to a significant extension of the inertial range of the capillary spectrum by more than one order of magnitude. A frequency power-law spectrum is then clearly observed on almost two decades. In the next part, we will explain the widening of the spectrum inertial range and the dependence of the crossover frequency on the upper fluid depth.

**Theoretical description.** – To interpret our experimental results, we consider gravity-capillary waves propa-

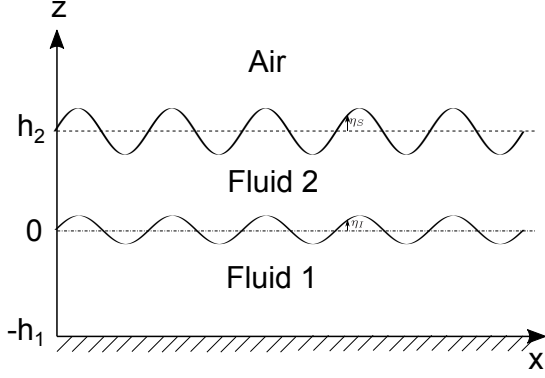


Fig. 5: Sinusoidal gravity-capillary waves propagating at the interface and at the free surface of two fluids of finite depths ( $h_1$  and  $h_2$  at rest). The upper surface is free. Case of in-phase deformations (mode +).

gating at both the interface and the free surface of two immiscible fluids of finite depths, the upper surface being free (fig. 5). The lower fluid is assumed to never emerge from the upper one. The dispersion relation of these waves can be found in textbooks [31,32] but only when the capillary effects are neglected. To our knowledge, the theoretical derivation of the dispersion relation taking into account both the gravity and capillary effects for a two-layer fluid of finite depths with free upper surface were obtained only quite recently [1, 13], as well as the one taking also into account the fluid viscosity effects [10]. In the following, we will use the inviscid dispersion relation. The experimental validity of this hypothesis will be checked *a posteriori* (see below).

Let a sinusoidal wave propagate along the  $x$ -axis with angular frequency  $\omega$  and wave vector  $k$  at the interface between both fluids, noticed 1 and 2, of finite depths (fig. 5). Fluid 1 is limited at the bottom by a rigid wall and fluid 2 is free at its surface. Experimentally, one has  $6 \leq kh_1 \leq 500$  and  $0.2 \leq kh_2 \leq 103$ . Let  $\eta_I$  be the wave height at the interface and  $\eta_S$  be the wave height at the free surface. The system is assumed invariant along the  $y$ -axis, and the flows incompressible and inviscid. The interface at rest is located at  $z = 0$ . The corresponding dispersion relation reads [1, 13]

$$a\omega^4 + b\omega^2 + c = 0 \quad (1)$$

with

$$\begin{cases} a = \rho_2 [\rho_1 + \rho_2 \tanh(kh_1) \tanh(kh_2)] \\ b = -\rho_1(\rho_2 gk + \gamma_S k^3) \tanh(kh_2) + \\ \quad \rho_2 (-\rho_1 gk - (\gamma_I + \gamma_S)k^3) \tanh(kh_1) \\ c = [\gamma_I \gamma_S k^6 + g(\rho_2(\gamma_I - \gamma_S) + \rho_1 \gamma_S) k^4 \\ \quad - \rho_2(\rho_2 - \rho_1)g^2 k^2] \tanh(kh_1) \tanh(kh_2) \end{cases} \quad (2)$$

Note that for  $h_1 = h_2 = \infty$ , Eqs. (1) and (2) are well reduced to the usual gravity-capillary dispersion relation between two infinite fluids with no free surface [32]

$$\omega^2(k) = \frac{\rho_1 - \rho_2}{\rho_1 + \rho_2} gk + \frac{\gamma_I k^3}{\rho_1 + \rho_2}. \quad (3)$$

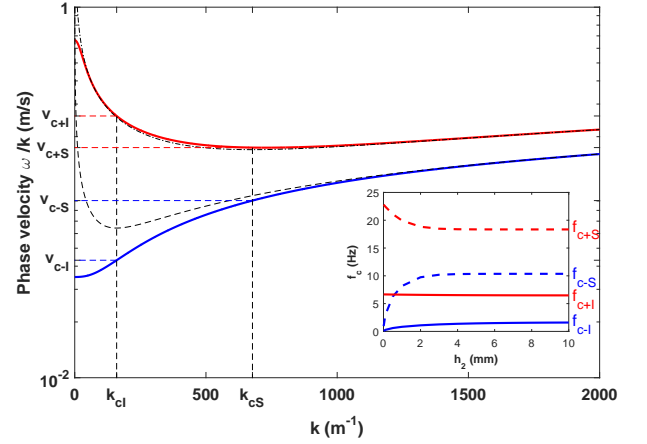


Fig. 6: (color online) Theoretical dispersion relation  $\omega/k$  vs.  $k$  for gravity-capillary waves in a two-layer fluid of finite depths from Eqs. (1) and (2). Red line: in-phase mode (mode +). Blue line: anti-phase mode (mode -).  $h_2 = 2$  mm. Black dashed line: Dispersion relation at the interface between the two same fluids but for infinite depths (Eq. 3). Black dash-dotted line: Dispersion relation at the free surface of a single fluid (2) of infinite depth (Eq. 4 with  $h_1 = \infty$ , replacing  $\rho_1$  and  $\gamma_I$  by  $\rho_2$  and  $\gamma_S$  respectively). Inset: Solid (resp. dashed) line: Crossover frequencies between capillary and gravity wave regimes at the interface (resp. at the free surface) for both modes as a function of  $h_2$ . Mode + (red). Mode - (blue).

For  $\rho_2 = 0$  and  $h_2 = \infty$ , Eqs. (1) and (2) lead to the usual gravity-capillary dispersion relation at the free surface of single fluid of finite depth [31]

$$\omega^2(k) = \tanh(kh_1) \left( gk + \frac{\gamma_I k^3}{\rho_1} \right). \quad (4)$$

The dispersion relation in the general case, Eqs. (1) and (2), have 4 solutions  $\omega^2(k) = \frac{-b \pm \sqrt{b^2 - 4ac}}{2a}$  among which only 2 are real, that are plotted in solid lines (blue and red) in fig. 6. We will call these solutions “mode +” and “mode -” according to the sign in the above expression of  $\omega^2(k)$ . Note that the mode + has a higher phase velocity than the mode - (semilog-y plot in fig. 6). Figure 6 also shows that even for a thin enough upper fluid layer (as small as 2 mm), the wave dispersion relation is constituted of two branches corresponding to the two propagating modes. This differs strongly from the dispersion relation for interfacial waves between two infinite fluids (see dashed line) or for surface waves on the surface a single infinite fluid (see dash-dotted line). The interfacial and free surface waves are indeed not independent but are coupled to each other by those two propagative modes. Both modes propagate at both interface and free surface. The ratio between the wave heights at the free surface (S) and the interface (I) reads [1]



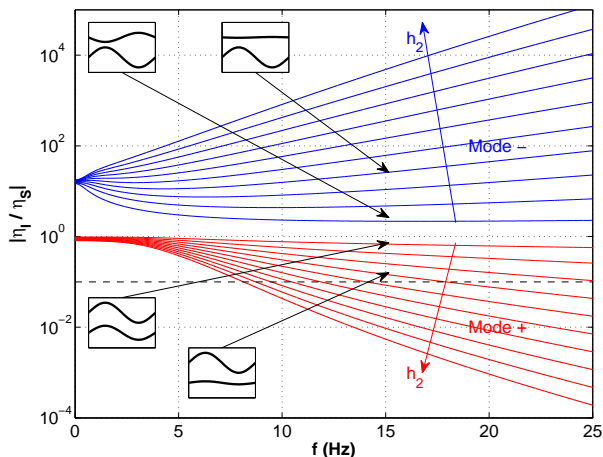


Fig. 7: (color online) Theoretical ratio from Eq. (5) between the interfacial and surface wave heights as a function of their frequencies, for different upper fluid depth  $h_2 = 1$  to 10 mm with a step of 1 mm (see arrows). Red lines: Mode +. Blue lines: Mode -. Dashed line:  $|\eta_I| = |\frac{\eta_S}{10}|$ . Insets show temporal evolutions of the surface and interfacial wave heights, for a fixed frequency  $f = 15$  Hz,  $h_2 = 1$  or 4 mm, and for both modes.

$$\frac{\eta_S}{\eta_I} = \frac{\sinh(kh_2)}{\rho_2} \times \left[ \rho_2 \coth(kh_2) + \rho_1 \coth(kh_1) - \frac{[(\rho_1 - \rho_2)g + \gamma_I k^2]k}{\omega^2(k)} \right]. \quad (5)$$

If  $\eta_S/\eta_I > 0$ , the waves at the interface and the ones at the free surface propagate in phase, corresponding to the mode + (also called barotropic [9] or zigzag [10] mode) as illustrated in Fig. 5. For  $\eta_S/\eta_I < 0$ , they propagate in antiphase corresponding to the mode - (also called varicose mode [10]).

The modulus of the wave height ratio  $|\eta_I/\eta_S|$  is plotted in fig. 7 as a function of the wave frequency for different depths  $h_2$ , for both modes. We first note that the surface wave height is higher than that of the interfacial wave height for the mode +, regardless  $h_2$ . On the other hand, for the mode -, the interfacial wave height is higher than that of the surface wave height, regardless  $h_2$ . Second, within our experimental frequency range ( $f \geq 6$  Hz) and for small  $h_2$ , wave heights at the interface and at the free surface is found to be of the same order for both modes, and are thus coupled (see insets of fig. 7). For large  $h_2$ , waves are uncoupled since the interface wave height is much smaller (resp. much higher) than that of the surface wave height for mode + (resp. mode -): waves can be thus considered to propagate only at the free surface for the mode + and only at the interface for the mode -. Note that this decoupling is as strong as the wave frequency is large. These features are shown in the insets of fig. 7 for a fixed wave frequency.

**Interpretation.** – Let us introduce the typical capillary lengths of the interface,  $l_{cI}$ , and of the free surface,  $l_{cS}$ . The corresponding wavenumbers are  $k_{cI} \equiv 1/l_{cI} = \sqrt{(\rho_1 - \rho_2)g/\gamma_I}$  and  $k_{cS} \equiv 1/l_{cS} = \sqrt{\rho_2 g/\gamma_S}$  ( $\lambda_{cI} \equiv 2\pi/k_{cI} \simeq 3.9$  cm ;  $\lambda_{cS} \equiv 2\pi/k_{cS} \simeq 0.9$  cm). Using the dispersion relation  $\omega(k)$ , those typical lengths correspond to 2 frequencies per mode:  $f_{c-I}$ ,  $f_{c-S}$  (mode -) and  $f_{c+I}$ ,  $f_{c+S}$  (mode +) as displayed in fig. 6 in the phase velocity space ( $v \equiv \omega/k$ ;  $k$ ) for a fixed depth  $h_2$ . Those frequencies correspond to the crossover frequencies between gravity and capillary wave regimes either at the interface (I) or at the free surface (S) for both modes (+ or -). The evolutions of these 4 frequencies with the upper fluid depth,  $h_2$ , are plotted in the inset of fig. 6. They are almost independent of  $h_2$  within our experimental range ( $h_2 \geq 2$  mm) and only  $f_{c+S}$  and  $f_{c-S}$  lie within our experimental frequency range ( $f \geq 6$  Hz).

Let us now interpret the experimental evolution of the crossover frequency  $f_t$  between gravity and capillary wave turbulence regimes when  $h_2$  is increased (see inset of fig. 4). As explained above, for small depths  $h_2$ , waves at the interface and at the free surface are coupled for both propagating modes + or -. The theoretical crossover frequency  $f_{c+S}$  at the free surface for the mode + is found to well describe the data for small enough depths  $h_2$  (see dashed line in the inset of fig. 4). When  $h_2$  is increased, this is no longer the case. Indeed, as also explained above, when  $h_2$  is increased, the waves propagating at the interface and at the free surface becomes progressively uncoupled for both modes: their relative heights  $|\eta_I/\eta_S|$  decreases strongly for the mode + or strongly increased for mode - (see fig. 7). We arbitrarily decide that waves become uncoupled when  $|\eta_I/\eta_S| \leq 1/10$  in the mode +, that is when the interface wave height becomes 10 times smaller than the free surface wave height. Interfacial waves can thus only propagate significantly on the other mode (mode -). This criterion corresponds to the dashed line in fig. 7. The intercepts of this dashed line and each solid line in fig. 7, for each depth  $h_2$ , thus give the frequencies  $f_{\text{un}}$  for which the interface and free surface waves of the mode + become uncoupled.  $f_{\text{un}}$  is then found to decrease with  $h_2$  in rough agreement with the experimental crossover frequency  $f_t$  at large  $h_2$  (see solid line in the inset of fig. 4).

To sum up, for small fluid depths  $h_2$ , the interface waves (that we measure) propagate on both modes and are coupled with surface waves. The crossover frequency between the gravity and capillary wave turbulence regimes observed on the spectrum,  $f_t$ , is linked to the value of  $f_{c+S}$  the capillary length at the free surface of the in-phase mode (mode +). The dependence of  $f_t$  on  $h_2$  is thus well described by  $f_{c+S}(h_2)$  until the interfacial and surface waves decouple for large enough  $h_2$ , that is for  $f_{\text{un}} < f_{c+S}$  (see inset of fig. 4).

**Time-scale separation.** – Let us now consider the typical time scales involved in our experiment. Weak turbulence theory assumes a time-scale separation  $\tau_l(f) \ll$

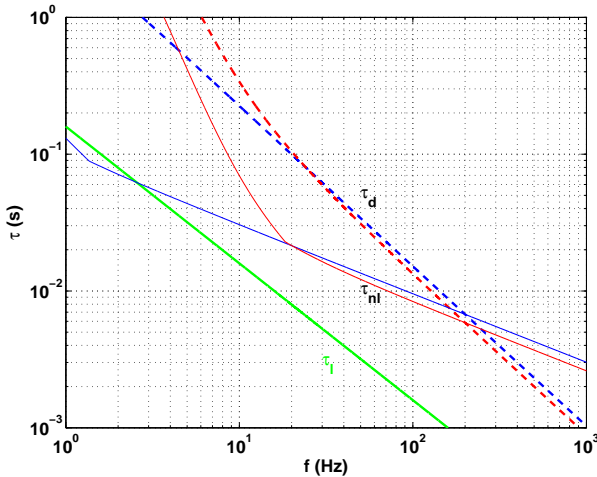


Fig. 8: (color online) Typical time scales as a function of the wave frequency. Thick solid (green) line:  $\tau_l = 1/\omega$ . Thin solid lines:  $\tau_{nl}$ . Dashed lines:  $\tau_d$ . Mode  $-$  (resp.  $+$ ) is shown in blue (resp. red).  $h_2 = 4$  mm.

$\tau_{nl}(f) \ll \tau_d(f)$ , between the linear propagation time,  $\tau_l$ , the nonlinear interaction time,  $\tau_{nl}$ , and the dissipation time,  $\tau_d$ . The linear propagation time is  $\tau_l = 1/\omega(k)$ . The dissipative time scale is linked to the viscous surface boundary layer, modeled by an inextensible infinitely thin film on the free surface, reading  $\tau_d = \frac{2\sqrt{2}}{k(\omega)\sqrt{\nu\omega}}$  [32, 33]. The kinematic viscosity of the two-layer fluid is  $\nu = \frac{\mu_1 \coth(kh_1) + \mu_2 \coth(kh_2)}{\rho_1 \coth(kh_1) + \rho_2 \coth(kh_2)}$  with  $\mu_1$  (resp.  $\mu_2$ ) the dynamic viscosity of the fluid beneath (resp. above) the interface [34]. We show in fig. 8 that the condition  $\tau_l(f) \ll \tau_d(f)$  is well satisfied in our experimental frequency range for both modes. It thus validates *a posteriori* the use here of an inviscid dispersion relation. Finally, for wave turbulence to take place, the typical time scale  $\tau_{nl}$  of nonlinear wave interactions has to satisfy  $\tau_l(f) \ll \tau_{nl}(f) \ll \tau_d(f)$ . For capillary waves,  $\tau_{nl}^c \propto k^{-3/4}$  [21, 35] while for gravity waves,  $\tau_{nl}^g \propto k^{-3/2}$  [35]. Since the prefactors of these laws are experimentally unknown,  $\tau_{nl}^c$  and  $\tau_{nl}^g$  are plotted in fig. 8 considering  $\tau_{nl}^c(f_{cut}) = \tau_d(f_{cut})$  at the cut-off frequency of the experimental capillary power-law spectrum ( $f_{cut} \simeq 200$  Hz for  $h_2=4$  mm - see fig. 4), and  $\tau_{nl}^g(f_t) = \tau_{nl}^c(f_t)$  at the experimental crossover frequency,  $f_t$ . Figure 8 shows that the time-scale separation is valid on the whole frequency range of our experiment. We also verified that this is true regardless our range of upper fluid depth  $h_2$ .

**Conclusion.** – In this paper, we studied gravity-capillary wave turbulence on the interface between two immiscible fluids with free upper surface. Waves propagate both at the interface and at the free surface [either in phase (mode  $+$ ) or in antiphase (mode  $-$ )], and this coupling depends strongly on the upper fluid depth. When this depth is increased, these two modes become progressively uncoupled, and we show that this decoupling explains most of the observations on the wave turbulence spectra. Indeed,

the crossover frequency between the gravity and capillary wave turbulence regimes is experimentally found to decrease by more than a factor 2 when the upper fluid depth is increased. At small depths, interfacial and surface waves are coupled, and this crossover is linked to the value of the capillary length at the free surface of the in-phase mode. At large enough depth, they become uncoupled when the interfacial wave heights of this mode become negligible with respect to the surface wave heights. Interfacial waves (that we measure) can thus only propagate significantly on the other mode. The crossover frequency is then well described by this decoupling criterion depending on the upper fluid depth. Finally, when the upper fluid is deep enough, the two modes are then fully uncoupled. This leads to the observation of a spectrum of purely capillary interfacial wave turbulence on two decades in frequency, fluids being of almost same density. This frequency range is comparable to what was previously observed at the interface between two immiscible deep fluids of almost equal densities with no upper free surface [36] or during micro-gravity experiments with a single fluid [37]. At last, this study may be useful to better understand nonlinear wave dynamics within a two-layer fluid in presence of surface and interfacial tensions such as oil spilling in oceanography and gravity-capillary solitary waves. The reported phenomenon is more general and should be shown up in other wave turbulence systems involving the coupling between surface and interfacial waves.

\*\*\*

We thank J. Servais for technical assistance. B. I. thanks CNRS for funding him as a one year postdoctoral research fellow. This work has been partially supported by ANR Turbulon 12-BS04-0005.

## REFERENCES

- [1] MOHAPATRA S. C., KARMAKAR D. and SAHOO T., *J. Eng. Math.*, **71** (2011) 253
- [2] JAMALI M., SEYMOUR B. and LAWRENCE G. A., *Phys. Fluids*, **15** (2003) 47-55
- [3] EKMAN V. W., *Norw. N. Polar Exped. 1893-1896: Sci. Results*, **5** (1904) 1-150
- [4] MERCIER M. J., VASSEUR R. and DAUXOIS T., *Nonlin. Processes Geophys.*, **18** (2011) 193-208
- [5] GRUE J., *Phys. Fluids*, **27** (2015) 082103
- [6] STAPLETON N.R., *Proc. Geosci. Remote Sensing Symposium, 1995, IGARSS '95*, **3** (1995) 1646-1648
- [7] WEI G., LU D. and DAI S., *Acta Mech. Sinica*, **21** (2005) 24-31
- [8] TROWBRIDGE J. H. and TRAYKOVSKI P., *J. Geophys. Res. Oceans*, **120** (2015) 5698-5709
- [9] PUCCI G., BEN AMAR M. and COUDER Y., *J. Fluid Mech.*, **725** (2013) 402
- [10] POTOTSKY A. and BESTEHORN M., *Phys. Rev. Fluids*, **1** (2016) 023901
- [11] POTOTSKY, A., BESTEHORN M., MERKT D. and THIELE U., *J. Chem. Phys.*, **122** (2005) 224711

- 
- [12] PÉRON N., BROCHARD-WYART F. and DUVAL H., *Langmuir*, **28** (2012) 15844-15852
- [13] WOOLDENDEN H. C. and PARAU E. I., *J. Fluid. Mech.*, **688** (2011) 528
- [14] KOROBKIN A., PARAU E. I. and VANDEN-BROECK J.-M., *Phyl. Trans. R. Soc. A*, **369** (2011) 2803-2812
- [15] FALCON E., *Discrete and Continuous Dynamical Systems - Series B*, **13** (2010) 819-840
- [16] ZAKHAROV V. E., LYOV V. and FALKOVICH G., *Kolmogorov Spectra of Turbulence I: Wave Turbulence* (Springer-Verlag, Berlin) 1992
- [17] S. NAZARENKO, *Wave Turbulence* (Springer-Verlag, Berlin) 2011
- [18] NEWELL A. C. and RUMPF B., *Annu. Rev. Fluid Mech.*, **43** (2011) 59
- [19] HASSELMANN K., *J. Fluid. Mech.*, **12** (1962) 481
- [20] BENNEY D. J. and NEWELL A. C., *J. Math. Phys.*, **46** (1967) 363
- [21] ZAKHAROV V. E. and FILONENKO N. N., *J. Appl. Mech. Tech. Phys.*, **8** (1967) 37
- [22] SHRIRA V. and NAZARENKO S. (Editors), *Advances in wave turbulence*, Vol. **83** (World Scientific, Singapore) 2013
- [23] ISSENMANN B., WUNENBURGER R., CHRAIBI H., GANDIL M. and DELVILLE J.-P., *J. Fluid. Mech.*, **682** (2011) 460.
- [24] ZHOU H., YAO Y., CHEN Q., LI G. and YAO S., *Appl. Phys. Lett.*, **103** (2013) 234102
- [25] FALCON E., AUMAÎTRE S., FALCÓN C., LAROCHE C. and FAUVE S., *Phys. Rev. Lett.*, **100** (2008) 064503.
- [26] FALCON E., LAROCHE C. and FAUVE S., *Phys. Rev. Lett.*, **98** (2007) 094503
- [27] COBELLI P., PRZADKA A., PETITJEANS P., LAGUBEAU G., PAGNEUX V. and MAUREL A., *Phys. Rev. Lett.*, **107** (2011) 214503.
- [28] DENISSENKO P., LUKASCHUK S. and NAZARENKO S., *Phys. Rev. Lett.*, **99** (2007) 014501.
- [29] ISSENMANN B. and FALCON E., *Phys. Rev. E*, **87** (2013) 011001(R).
- [30] DEIKE L., MIGUEL B., GUTIÉRREZ P., JAMIN T., SEMIN B., BERHANU M., FALCON E. and BONNEFOY F., *J. Fluid Mech.*, **781** (2015) 196.
- [31] LANDAU L. and LIFSHITZ E., *Mécanique des fluides* (MIR) 1989, p. 62.
- [32] LAMB L. H., *Hydrodynamics* (Cambridge University Press) 1916
- [33] DEIKE L., BERHANU M. and FALCON E., *Phys. Rev. E*, **85** (2012) 066311.
- [34] KUMAR K. and TUCKERMAN L. S., *J. Fluid Mech.*, **279** (1994) 49.
- [35] DEIKE L., *Études expérimentales et numériques de la turbulence d'ondes de surface* (PhD, Université Paris Diderot - Paris 7) 2013, sect. 2.4.1.
- [36] DÜRING G. and FALCÓN C., *Phys. Rev. Lett.*, **103** (2009) 174503
- [37] FALCÓN C., FALCON E., BORTOLOZZO U. and FAUVE S., *EPL*, **86** (2009) 14002